Effects of Perforated Partition Plate on Mixing Characteristics of Horizontal Stirred Vessel

KOJI ANDO
MINORU SHIRAHIGE
TAKASHI FUKUDA
and
KAZUO ENDOH

Department of Chemical Engineering
Muroran Institute of Technology
Muroran 050, Japan

To reduce backmixing in the flow-type horizontal stirred vessel, a perforated partition plate was attached and the effects of shape of plate on the mixing characteristics were studied under various operating conditions. Results were analyzed in terms of mixing models to evaluate the extent of preventing backmixing. It enabled us to estimate the extent of back flow at the perforated partition plate from power consumption.

SCOPE

The purpose of the present study is to clarify the effects of the shape of perforated plate attached inside a flow-type horizontal stirred vessel under various operating conditions upon reducing liquid backmixing.

Kirk and Othmer (1951) and Ullmann (1928) showed a horizontal stirred vessel as a gas-liquid contactor for production of sodium formate from carbon monoxide and aqueous caustic soda. Ganz et al. (1958) carried out absorption experiments with various gas-liquid systems and observed that the horizontal stirred vessel equipped with a deformed circular plate as an impeller had high absorption capability. Recent studies on horizontal stirred vessels include those carried out by Ando et al. (1972), Misaka (1967), Sasaki (1971), Takeuchi et al. (1976), and Tamaki et al. (1974, 1975). In these studies, effects of the operating conditions, types of impeller, and flow behavior on the gas-liquid contact in the vessel have been examined. Power consumption was also examined by Ando et al. (1971a, 1978), Misaka (1967), and Tamaki and Ito (1973). In the foregoing studies, however, no consideration was given to the use of a partition plate as a means to reduce backmixing.

Fukuda et al. (1976) studied desorption of hydrogen cyanide from waste water using a commercial horizontal stirred vessel (1 m in diameter and 2 m in length) in a gas-liquid flow system. The apparatus used had a large contact area for its volume, and its was possible to control flow rates of gas and liquid separately. Even though the apparatus was found to desorb hydrogen cyanide effectively, they suggested the necessity of improving the liquid mixing characteristics since the liquid mixing under the conditions employed was close to complete mixing. Ando et al. (1971b, 1974) studied the effects of various operating conditions upon mixing time and residence time distribution, using a vessel without a perforated partition plate. No other report has been published to the present author's knowledge, on the mixing characteristics of a horizontal stirred vessel.

CONCLUSIONS AND SIGNIFICANCE

Liquid mixing in the present apparatus would be approximated adequately by a backmixing model consisting of completely mixed cells separated by a perforated partition plate and impellers. Based on this model, an equation $u_p' = Q_p - u/2$ was found to hold for the back-flow rate at the plate (u_p'), the liquid flow rate (u) and the rate of exchange between two cells separated by the plate (Q_p). The relation holds for a wide range of operating conditions, perforated plate shapes, and apparatus of various size. The values of Q_p were estimated from the power consumption.

Further, the partition plates composed of two parallel, thin, perforated plates were as good as or better than that of the single thick plate with long flow path.

A horizontal stirred vessel effectively mixes gas and liquid with rotating impeller, installed on a horizontal shaft, at the gas-liquid interface.

Most of the research reports on horizontal stirred vessels are concerned with the relationships among the gas-liquid contact, power consumption, types of impeller, and operating conditions (Ando et al., 1971a, 1972, 1978; Ganz, 1958; Misaka, 1967; Sasaki, 1971; Takeuchi et al., 1976; Tamaki and Ito, 1973; and Tamaki et al., 1974, 1975). Few reports have been published on mixing characteristics of horizontal stirred vessels.

Ando et al. (1971b, 1978) studied the relationship among operating conditions, mixing time of liquid, and residence time

Correspondence concerning this paper should be addressed to K. Ando. T. Fukuda is with Government Industrial Development Laboratory, Hokkaido, Sapporo 061-01. K. Endoh is with the Department of Chemical Process Engineering, Hokkaido University, Sapporo 060.

0001-1541-81-4370-0599-$2.00.

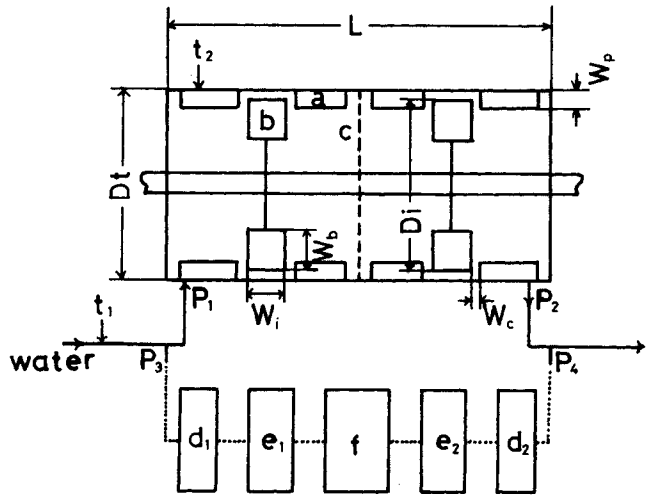

Figure 1. Schematic of the apparatus.

distribution. When a horizontal stirred vessel, used in a flow system, is operated under the condition that mean residence time of liquid is relatively long, liquid mixing in the vessel approaches complete mixing. Hence, the mixing characteristics must be improved for efficient mass transfer between gas and liquid (Fukuda et al., 1976).

In the present study, we attached a perforated plate inside a horizontal stirred vessel to reduce backmixing of liquid in a flow system operation and, using various size of apparatus, examined the effects of plate shape and operating conditions on the partition effect. A model for mixing in a horizontal stirred vessel equipped with a perforated partition plate was presented. A procedure to estimate the liquid mixing characteristics of the apparatus based on this model was given.

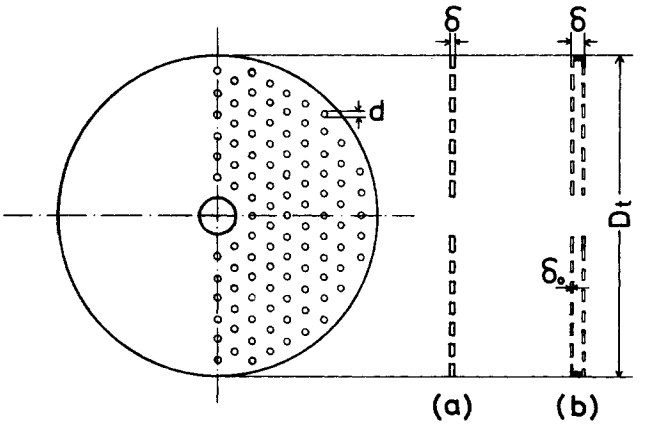

Figure 2. Perforated copper, polyethylene and acrylic plates in an equilateral triangle arrangement.

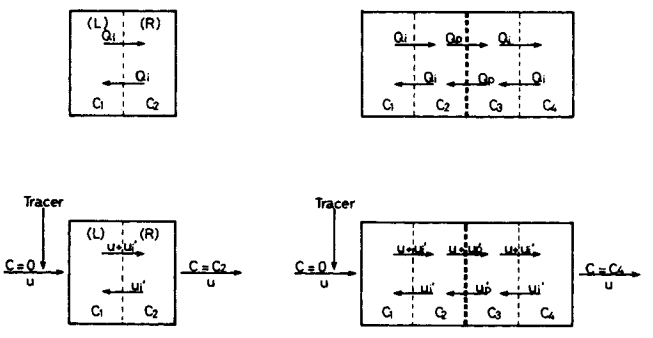

Figure 3. Mixing models for horizontal stirred vessels.

APPARATUS AND EXPERIMENTAL PROCEDURE

A schematic diagram of the apparatus used is shown in Figure 1. Two geometrically similar cylinders (0.15 and 0.23 m in diameter) equipped with four baffle plates at the top, bottom, left and right of the inside wall, were used as the horizontal vessel. In the center of the vessel was attached a perforated partition plate. In the center of the shaft of each cell, separated by the plate, was installed a four-blade turbine impeller. The shapes and principal dimensions of the stirred vessel, impeller, and baffle plate are shown in the diagram; they are practically the same as those used by Ando et al. (1974). Copper, polyethylene and acrylic plates, with thickness 1×10^{-4} to 3×10^{-3} m, were perforated in an equilateral triangle arrangement as shown in Figure 2. Number of holes was either 12, 75, 192, or 300. Diameters of hole ranged between 1.4×10^{-3} and 1×10^{-2} m. The partition plates composed of two perforated thin-plates as shown in Figure 2(b) were also examined. They were arranged parallel at a short distance with their hole positions slightly staggered. Open area ratio γ, hole number m, hole diameter d and vessel diameter D_t are related by an equation $\gamma = m \cdot d^2/D_t^2$. Throughout this study, a flow system was adopted only for the liquid, and the mixing characteristics of the liquid were determined by delta response method. A potassium chloride solution was injected at p_5 as a tracer. The tracer concentrations at p_3 of the inlet and p_4 of the outlet tube were followed by means of electric resistance of the liquid using bridges with two platinum electrodes and recorded simultaneously on a two-pen recorder.

The horizontal stirred vessel with baffle plate has the large absorption capability, when the vessel is approximately half filled with liquid (Ando et al., 1972). The present work was conducted in the liquid ratio ϵ(ratio of volume of liquid to volume of vessel) ranging from 0.4 to 0.6.

MIXING MODELS AND BACK FLOW RATE AT PERFORATED PARTITION PLATE u_p'

Mixing Models

The mixing models proposed by Ando et al. (1974) for horizontal stirred vessels with an impeller, but without a perforated partition plate, are shown in Figure 3(a) and (b). For batch vessel, mixing is controlled by liquid exchange rate Q_i between the two completely mixed cells separated by an impeller, as shown in Figure 3(a). On the other hand, a model consisting of two completely mixed cells with back flow rate u_i', Figure 3(b) describes mixing in the flow system.

For the present case where the plate is attached between two impellers, two foregoing models connected in series [Figures 3(c) and (d)] appear appropriate. That is, if a treatment similar to that of Ando et al. (1974) is applicable here, the liquid mixing in the present flow system should be adequately described by a model consisting of four completely mixed cells separated by two impellers and a perforated plate, with back flow rate u_i' in the vicinity of each impeller and back flow rate u_p' at the plate. Thus, the mixing characteristics of the apparatus are given by Eqs. 1 and 2:

$$\beta_p \equiv u_p'/u \tag{1}$$

$$\beta_i \equiv u_i'/u \tag{2}$$

where β_p means the partition effect of the perforated plate and β_i the mixing effect of a vessel without the plate. According to the previous study (Ando et al., 1974), β_i is estimated from power consumption.

Based on the back mixing model of Figure 3(d), the material balance is given by Eqs. 3 to 6. When the tracer is injected at time $\theta = 0$, the concentration at time θ of the tracer for each cell are C_1, C_2, C_3 and C_4:

First cell:

$$\frac{V}{4}\frac{dC_1}{d\theta} = C_2u_i' - C_1(u + u_i') \tag{3}$$

Second cell:

$$\frac{V}{4}\frac{dC_2}{d\theta} = C_3u_p' - C_2(u + u_i' + u_p') + C_1(u + u_i') \tag{4}$$

Third cell:

$$\frac{V}{4}\frac{dC_3}{d\theta} = C_4u_i' - C_3(u + u_i' + u_p') + C_2(u + u_p') \quad (5)$$

Fourth cell:

$$\frac{V}{4}\frac{dC_4}{d\theta} = -C_4(u + u_i') + C_3(u + u_i') \quad (6)$$

Since $C_1 = 4$ and $C_2 = C_3 = C_4 = 0$ at $\theta = 0$, the residence time distribution function $E(\phi)$ is given by Eq. 7:

$$E(\phi) = 16(1 + \beta_i)^2\sqrt{\frac{1 + \beta_p}{\beta_p}}\left\{\frac{\exp(D + B)\phi}{B^2 + 2(\sqrt{\beta_p(1 + \beta_p)} - \beta_p)B} + \frac{\exp(D - B)\phi}{B^2 - 2(\sqrt{\beta_p(1 + \beta_p)} - \beta_p)B} - \frac{\exp(C + A)\phi}{A^2 - 2(\sqrt{\beta_p(1 + \beta_p)} + \beta_p)A} - \frac{\exp(C - A)\phi}{A^2 + 2(\sqrt{\beta_p(1 + \beta_p)} + \beta_p)A}\right\} \quad (7)$$

where

$$A = 2\sqrt{4\beta_i(1 + \beta_i) + 2\beta_p(1 + \beta_p) - \beta_p(1 - 2\sqrt{\beta_p(1 + \beta_p)})}$$

$$B = 2\sqrt{4\beta_i(1 + \beta_i) + 2\beta_p(1 + \beta_p) - \beta_p(1 + 2\sqrt{\beta_p(1 + \beta_p)})}$$

$$C = 2[-2(1 + \beta_i) - \beta_p - \sqrt{\beta_p(1 + \beta_p)}]$$

$$D = 2[-2(1 + \beta_i) - \beta_p + \sqrt{\beta_p(1 + \beta_p)}]$$

and where $\phi(\equiv\theta/\theta_T)$, $\theta_T(\equiv V_1/u)$ and V_1 are dimensionless residence time, mean residence time and total volume of liquid in the vessel, respectively.

Calculation of Back Flow Ratio at Perforated Partition Plate $\beta_p(\equiv u_p'/u)$

Figure 4 shows an example of response curve. Curve A illustrates a concentration change on the inlet side, and curve B that on the outlet side. The starting time ($\theta = 0$) is taken when the tracer concentration on the inlet side begins to tail. θ_s in Figure 4 means the difference between the starting position of curve A and that of B. θ_{max} is the time corresponding to the maximum of the response curve. The time needed for the liquid to pass through the tube sections (p_3-vessel, p_4-vessel in Figure 4) is negligible compared to θ_{max}.

Circles in Figure 4 are the values calculated from Eq. 7, using $\beta_p = 0.9$ and $\beta_i = 6$. Figure 4 indicates that the experimental values agree quite well with the calculated ones. Under other operating conditions, agreement between experimental and calculated values was also satisfactory. Therefore, in the following analysis, back flow ratio $\beta_p(\equiv u_p'/u)$ and back flow rate u_p' at the plate were determined using experimental dimensionless time $\phi_{max}(\equiv\theta_{max}/\theta_T)$ and $\beta_p/\beta_i - \phi_{max}$ relationship of Figure 5. The values for β_i were obtained from Eq. 24, as will be discussed later.

Relation between Back Flow u'_p at Perforated Partition Plate and Liquid Flow u

Figure 6 shows the relationship between experimental back flow rate u_p' at the plate and liquid flow rate u. The rate u_p' decreases with an increase in u, giving a slope of approximately $-1/2$. At a constant liquid flow rate, u_p' increases as the speed of the impeller rotation n, the liquid-vessel volume ratio ϵ, and the open area ratio of the plate γ increase. On the other hand, u_p' decreases as the thickness of the perforated plate δ increases. A straight line with a slope of $-1/2$ is drawn for each set of data and its intercept at $u = 0$ is taken as u_{p0}':

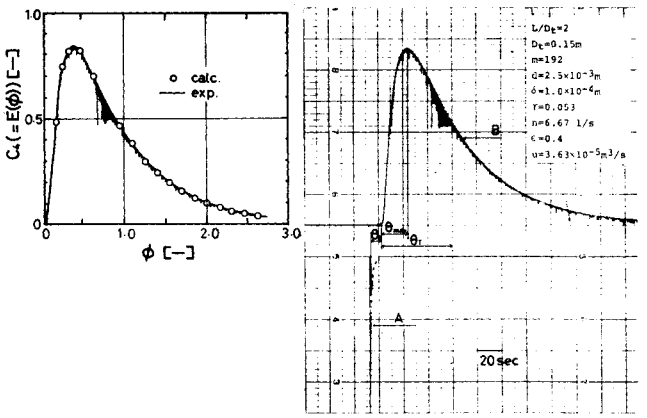

Figure 4. Example of response curve.

$$u_p' = u_{p0}' - \frac{1}{2}u \quad (8)$$

The plots of u_p'/u_{p0}' against u/u_{p0}' are shown in Figure 7. Hence, Eq. 8 holds for a wide range of operating conditions, perforated plate shapes, and apparatus scales.

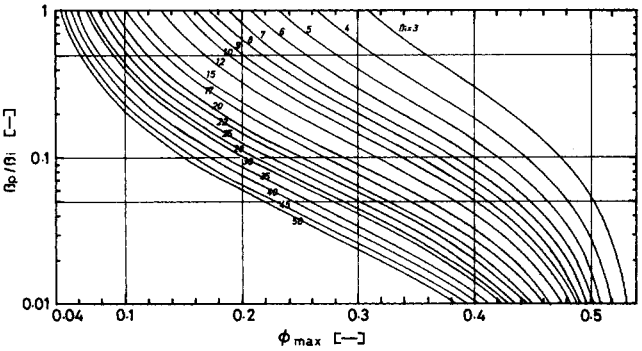

Figure 5. Relationship of β_i and $\beta_p/\beta_i - \phi_{max}$.

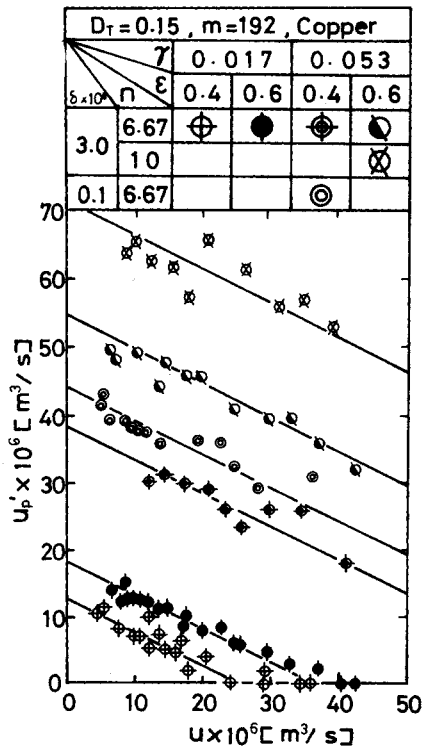

Figure 6. Relationship between experimental back flow rate and liquid flow rate.

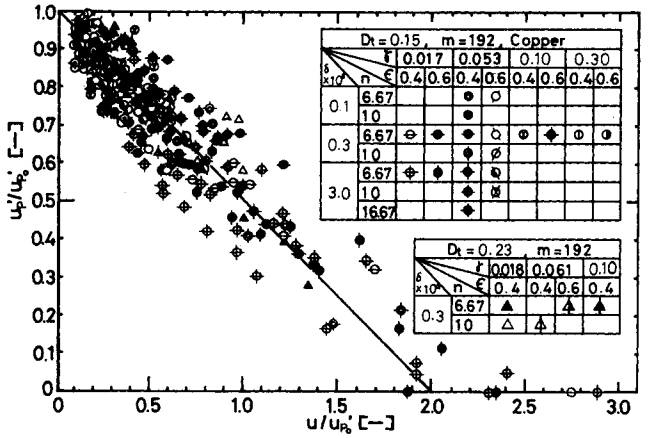

Figure 7. Plots of u_p/u_{po} against u/u_{po}.

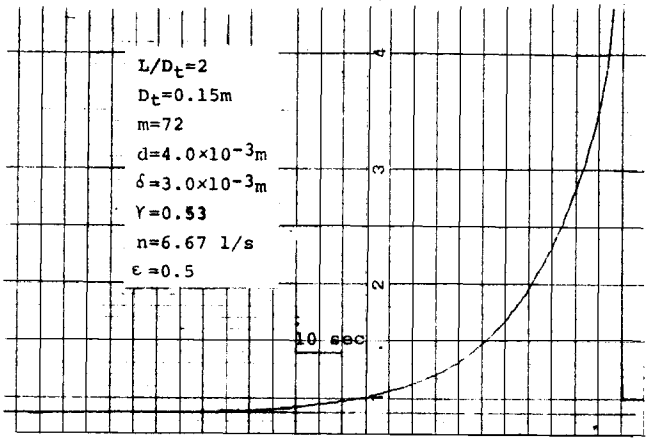

Figure 8. Relationship between pen position and time.

EXCHANGE RATE RATIO Q_p/Q_i OF BATCH OPERATION

Measurements of Exchange Rate Ratio Q_p/Q_i

The same method as described in the previous report (Ando et al., 1971b) was employed to measure the mixing time of batch vessel. Namely, two pairs of platinum electrode were installed at p_1 and p_2, i.e. two bottom positions, Figure 1. The electric resistance of liquid at the electrodes was used as the resistance of bridge circuit. Solution of potassium chloride was injected from above p_1 as a tracer, and its concentration change with time was followed by measuring electric resistance. Under the experimental conditions employed, the response of recording pen changed proportionately to the difference in tracer concentrations between the electrodes.

Figure 8 illustrates the relationship between the pen position and time. The pen positions relative to that after a sufficiently long period were measured at each time θ. The displacement, or the concentration difference between p_1 and p_2, $(C_1 - C_4)$, decreases exponentially with time and was approximated by the following equation:

$$C_1 - C_4 = K \exp(-\theta/\tau) \tag{9}$$

In the present study, mixing time θ_M is defined as 4τ corresponding to 98% equilibration.

The exponential relationship of Eq. 9 may be interpreted based on the mixing model of Figure 3(c). The model presupposes that the vessel consists of completely mixed cells separated by the impellers and the plate and that the liquid exchange rate across the two adjacent cells controls the over-all mixing. If the exchange rate at the impeller and that at the plate are designated as Q_i and Q_p, respectively, the material balance for each cell as to tracer concentration is expressed as follows:

First cell:

$$\frac{V}{4}\frac{dC_1}{d\theta} = Q_i(C_2 - C_1) \tag{10}$$

Second cell:

$$\frac{V}{4}\frac{dC_2}{d\theta} = Q_i(C_1 - C_2) + Q_p(C_3 - C_2) \tag{11}$$

Third cell:

$$\frac{V}{4}\frac{dC_3}{d\theta} = Q_p(C_2 - C_3) + Q_i(C_4 - C_3) \tag{12}$$

Fourth cell:

$$\frac{V}{4}\frac{dC_4}{d\theta} = Q_i(C_3 - C_4) \tag{13}$$

Since $C_1 = 1$ and $C_2 = C_3 = C_4 = 0$ at $\theta = 0$, the difference in concentration between cell 1 and cell 4, $\Delta C(=C_1 - C_4)$, is obtained as follows:

$$\Delta C = \frac{Q_i^2}{2(Q_i^2 + Q_p^2 - Q_p\sqrt{Q_i^2 + Q_p^2})} \exp\left\{\frac{-4(Q_i + Q_p - \sqrt{Q_i^2 + Q_p^2})}{V_1} \cdot \theta\right\} + \frac{Q_i^2}{2(Q_i^2 + Q_p^2 + Q_p\sqrt{Q_i^2 + Q_p^2})} \exp\left\{\frac{-4(Q_i + Q_p + \sqrt{Q_i^2 + Q_p^2})}{V_1} \cdot \theta\right\} \tag{14}$$

If θ is sufficiently large, the first term of Eq. 14 becomes large compared with the second term. Thus, in the region where the second term is negligible, mixing time θ_M and relaxation time τ would be approximated by the following equation:

$$\theta_M \equiv 4\tau = \frac{V_1}{Q_i + Q_p - \sqrt{Q_i^2 + Q_p^2}} \tag{15}$$

In Table 1 are shown the relationship between ΔC of Eq. 14 and dimensionless time $\psi(\equiv\theta/\theta_M)$ and that between the first term of Eq. 14 and ψ. Table 1 shows evidently that the second term of

TABLE 1. RELATION BETWEEN Δ C CALCULATED FROM EQUATION (14) AND FIRST TERM OF EQUATION (14) FOR VARIOUS ψ AND Q_p/Q_i

ψ ($\equiv\theta/\theta_M$) \ Q_p/Q_i	1.0		0.3		0.1	
	Δ C	1st term	Δ C	1st term	Δ C	1st term
0.01	0.9361	0.8201	0.8655	0.6184	0.7138	0.5282
0.02	0.8798	0.7879	0.7655	0.5942	0.5840	0.5075
0.05	0.7445	0.6988	0.5841	0.5270	0.4555	0.4501
0.1	0.5864	0.5722	0.4406	0.4315	0.3636	0.3685
0.2	0.3849	0.3835	0.2895	0.2892	0.2470	0.2470
0.5	0.1155	0.1155	0.0871	0.0871	0.0744	0.0744
1.0	0.0156	0.0156	0.0118	0.0118	0.0101	0.0101

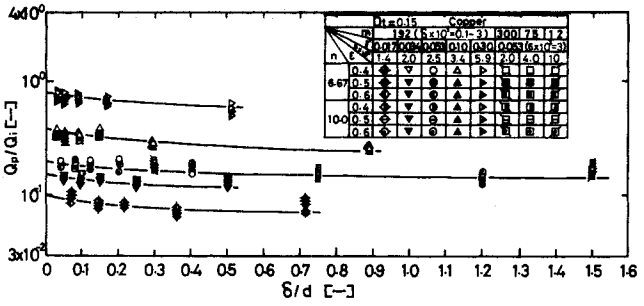

Figure 9. Ratio of experimentally determined exchange rate vs. ratio of the thickness to the hole diameter of perforated partition plate.

Eq. 14 will be neglected in the region where $\psi > 0.1$.

Analogously, mixing time θ_{M_1}, of the single-impeller model shown in Figure 3(a), ($L/D_t = 1.0$) is expressed as follows:

$$\theta_{M_1} = \frac{V_1/2}{Q_i} \tag{16}$$

If exchange rate Q_i at the impeller is assumed to remain unaffected by the presence of a perforated partition plate, that is, if Q_i of Figure 3(a) is equal to Q_i of Figure 3(c), the following equation is obtained from Eqs. 15 and 16.

$$\frac{Q_p}{Q_i} = \frac{2\theta_{M_1}(\theta_M - \theta_{M_1})}{\theta_M(\theta_M - 2\theta_{M_1})} \tag{17}$$

Eq. 17 means that the exchange rate ratio Q_p/Q_i can be determined experimentally by measuring mixing time θ_M of a vessel with the perforated partition plate, Figure 3(c), and mixing time θ_{M_1} of a cell equipped only with an impeller, Figure 3(a).

Relationship between Exchange Rate Ratio Q_p/Q_i and Operating Conditions and Shape of Perforated Partition Plate

The relationship between experimentally determined exchange rate ratio Q_p/Q_i and the ratio of thickness to hole diameter δ/d of perforated partition plate is shown in Figure 9. For the same plate, Q_p/Q_i stays nearly even if operating conditions (n, ϵ) were changed. The relationship between Q_p/Q_i and δ/d does not change significantly with the plate shapes (δ, d and m), as long as the open area ratio γ remains constant. Thus, at a constant open area ratio, Q_p/Q_i decreases with an increase in δ/d and reaches a constant value regardless of operating conditions. Further, if δ/d is kept constant, Q_p/Q_i increases with an increase in γ. The dependence of Q_p/Q_i on γ and on δ/d was obtained experimentally as shown in Figure 10. The solid line drawn follows the following equation:

$$\frac{Q_p}{Q_i} = \frac{2\gamma^{0.73}}{1 + 0.4(\delta/d)^{0.5}} \tag{18}$$

where $0.017 < \gamma < 0.30$ and $0.03 < \delta/d < 2.15$. Experimental results obtained with apparatus of various size are now correlated in terms of Eq. 18 with an accuracy to ±20%.

Haug (1971) pointed out that, with a multistage stirred-type counterflow contactor, the wettability and interfacial tension affect the partition effect. For this reason, we examined the partition effects of perforated plates made of polyethylene and acrylic resins. A part of the results are shown in Figure 10. No significant difference is observed between these perforated plates and that made of copper.

Figure 10 also shows a part of the exchange rate ratio Q_p/Q_i measured with a parallel set of two perforated thin-plates, Figure 2(b). The measured values are in the vicinity of the broken line and indicate a deviation of −20% from the empirical equation (Eq. 18) derived with single perforated plate, Figure 2(a). Q_p/Q_i of the parallel set of two perforated plates is affected by thickness δ_0 of the perforated plate used; even if the total thickness δ is kept constant, Q_p/Q_i decreases with an increase in δ_0.

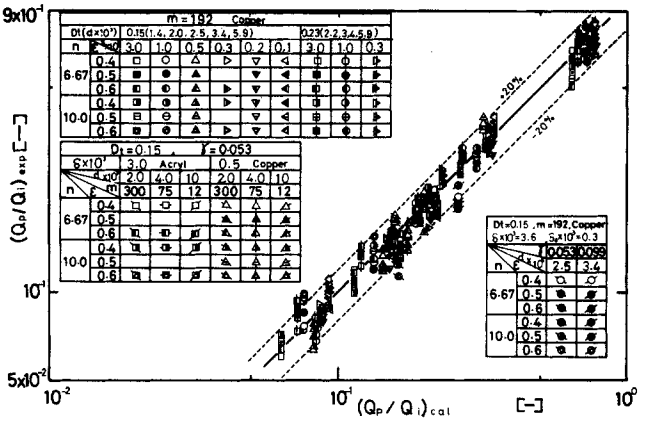

Figure 10. Partition effects of perforated plates made of copper and acrylic resin.

However, if δ_0/d is equal to or less than 0.1, Q_p/Q_i follows Eq. 18. Namely, the partition effect of the parallel set of two perforated thin-plates is as good as or better than that of single perforated plate of equal thickness δ. Therefore, if the thickness of a single perforated plate becomes excessively large as a result of scale-up under the geometrical similarity rule, use of partition plate composed of two perforated thin-plates is advantageous.

Relation between Back Flow u_p' and Exchange Rate Q_p

As is evident from mixing models, Figure 3(c) and (d), the back flow u_{p_0}', obtainable by substituting zero for u in Eq. 8, is equal to the exchange rate Q_p of batch process. Therefore, what has been found with the exchange rate Q_p should be applicable to u_{p_0}' in Eq. 8 as well. If one put Q_p in place of u_{p_0}', Eq. 8 becomes:

$$\frac{u_p'}{u}\ (\equiv\beta_p) = \frac{Q_p}{u} - \frac{1}{2} \tag{19}$$

From Eqs. 18 and 19, one obtains:

$$\frac{u_p'}{u}\ (\equiv\beta_p) = \frac{2\gamma^{0.73}}{1 + 0.4(\delta/d)^{0.5}} \cdot \frac{Q_i}{u} - \frac{1}{2} \tag{20}$$

According to the previous report (Ando et al., 1974) on the mixing characteristics of horizontal stirred vessel without a perforated plate, Q_i/u in Eq. 20 is given by the Eqs. 21 and 22:

$$\frac{u_i'}{u}\ (\equiv\beta_i) = K \cdot \frac{\theta_{T_1}}{\theta_{M_1}} \left(= K \cdot \frac{Q_i}{u}\right) \tag{21}$$

$$K = 0.85 \text{ and } \beta_i > 1.5$$

$$\frac{1}{n\theta_M}\frac{L}{D_t} = 2.3 \times 10^{-2}\left(\frac{N_p}{\epsilon}\right)^{0.7} \tag{22}$$

In Eqs., θ_{M_1} and θ_{T_1} denote mixing time and mean residence time of a vessel without a perforated plate, respectively, and N_p means the power number. The value of K in Eq. 21, has been determined experimentally, using a relationship that $u_i' = KQ_i$, regardless of the magnitude of u. If Q_i/u is sufficiently small, however, the effect of u on back flow u_i' cannot be neglected. Thus, Eq. 21 holds only when $\beta_i > 1.5$ or $Q_i/u > 2$. The same argument on Eq. 19 gives the effect of flow rate u on the relationship between back flow u_i' and exchange rate Q_i in the form of Eq. 23:

$$\frac{u_i'}{u}\ (\equiv\beta_i) = \frac{Q_i}{u} - \frac{1}{2} \tag{23}$$

Eq. 23 holds for the data of the previous report even if Q_i/u ($=\theta_{T_1}/\theta_{M_1}$) is small. Thus, in the present study, the values of β_i were calculated according to the following equation obtained from Eqs. 22 and 23.

$$\frac{u_i'}{u}\ (\equiv\beta_i) = 2.3 \times 10^{-2}\frac{n\theta_T}{(L/D_t)}\left(\frac{N_p}{\epsilon}\right)^{0.7} - \frac{1}{2} \tag{24}$$

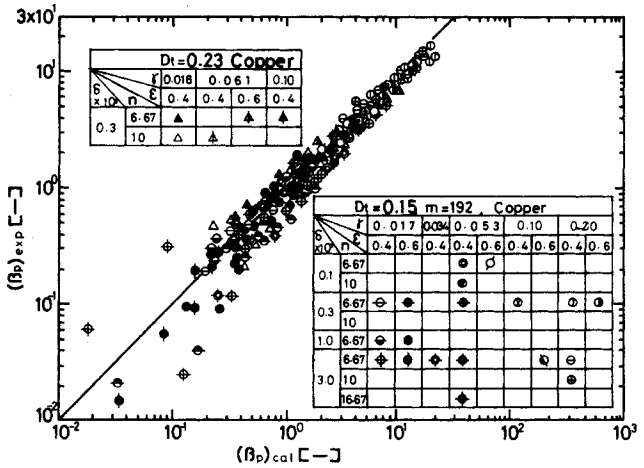

Figure 11. Experimentally obtained back flow ratio.

Figure 11 shows plots of experimentally obtained back flow ratio β_p at the perforated partition plate against the right-hand side of Eq. 20. A good correlation exists for a wide range of operating conditions. Essentially the same correlation was obtained with the partition plate composed of two perforated thin-plates.

The results obtained above clearly indicate that the back flow β_p at the perforated partition plate of the present apparatus is estimated from power number N_p and Eq. 20.

CONCLUSIONS

For the purpose of improving the liquid mixing characteristics of flow-type horizontal stirred vessel, perforated partition plate was attached to the inside of the vessel. The effects of the plate shape (hole diameter d, open area ratio γ, thickness δ) and operating conditions (flow rate u, rotational speed of impeller n, ratio of volume to vessel volume ϵ) on the partition efficiency were studied using apparatus of various size. Results were analyzed in terms of several mixing models, and the effect of the perforated partition plate on backmixing reduction was evaluated.

The mixing of liquids inside the present apparatus would be approximated adequately by a backmixing model consisting of completely mixed cells separated by the partition plate and impellers. From the mixing models, a relationship ($u_p' = Q_p - u/2$) was derived among the back flow u_p' at the partition plate, the exchange rate Q_p at the partition plate of a batch vessel, and the liquid flow rate u. The relationship was subsequently confirmed by experiments. The dependence of the plate shape on the exchange rate Q_p is calculated in Eq. 18.

ACKNOWLEDGMENT

The authors would like to thank J. Sugita for his advice, and M. Sakakibara, M. Miura and T. Shiraiwa for their assistance.

NOTATION

c = concentration
c_j = concentration of KCl solution in jth cell
D_i = diameter of impeller
D_t = diameter of horizontal stirred vessel
d = diameter of hole in perforated plate
$E(\phi)$ = distribution function for residence time
g = acceleration of gravity
L = length of horizontal stirred vessel
m = number of holes in perforated plate
n = rotational speed of impeller
N_{Fr} = Froude number ($=n^2D_i/g$)
N_p = Power number ($=P/\rho n^3D_i^5$)
P = power consumption
Q_i = exchange rate of liquid between 1st and 2nd cell or 3rd and 4th cell (at impeller)
Q_p = exchange rate of liquid between 2nd and 3rd cell (at partition plate)
u = net volumetric flow rate
u_i' = back flow rate of liquid between 1st and 2nd cell or 3rd and 4th cell (at impeller)
u_p' = back flow rate of liquid between 2nd and 3rd cell (at partition plate)
u_{p0}' = extrapolated value of u_p' obtained by putting $u = 0$ in Eq. 8
V = volume of horizontal stirred vessel
V_1 = volume of liquid in horizontal stirred vessel

Greek Letters

β_i = back flow ratio at impeller ($=u_i'/u$)
β_p = back flow ratio at partition plate ($=u_p'/u$)
γ = open area ratio of perforated plate
δ = thickness of partition plate
δ_o = thickness of perforated plate which composes the combined partition plate shown in Figure 2(b)
ϵ = ratio of volume of liquid to volume of horizontal stirred vessel ($=V_1/V$)
θ = time
θ_M = time for sufficient mixing
θ_T = mean residence time of liquid ($=V_1/u$)
τ = relaxation time of mixing
ϕ = dimensionless time ($=\theta/\theta_T$)
ϕ_{max} = dimensionless time when $E(\phi)$ has its maximum value
ψ = dimensionless time ($=\theta/\theta_M$)

LITERATURE CITED

Ando, K., H. Hara, and K. Endoh, "Behavior of Flow and Power Consumption of Horizontal Stirred Vessel," *Kagaku Kōgaku*, **35**, No. 4, 466 (1971a); *International Chem. Eng.*, **11**, 736 (1971a).

Ando, K., H. Hara, and K. Endoh, "On Mixing Time in Horizontal Stirred Vessel," *ibid*, **35**, 806 (1971b).

Ando, K., H. Tabo, and K. Endoh, "Effect of Baffle Plate on Absorption Rate of Gas in Batch Horizontal Stirred Vessel," *J. Chem. Eng. of Japan*, **5**, 193 (1972).

Ando, K., M. Goto, J. Sugita, T. Fukuda, and K. Endoh, "Torque of Drive Shaft in Horizontal Stirred Vessel," *Kagaku Kōgaku Ronbunshu*, **4**, 154 (1978).

Ando, K., T. Fukuda, and K. Endoh, "On Mixing Characteristics of Horizontal Stirred Vessel with Baffle Plate," *Kagaku Kōgaku*, **38**, 460 (1974).

Fukuda, T., K. Ando, T. Sato, and K. Endoh, "Performance Test of Commercial Size Horizontal Stirred Vessel for Stripping Waste Water Containing Hydrogen Cyanide," *Japan Kogyo Yosui*, No. 219, 19 (1976).

Ganz, S. N., and M. A. Lokshin, 'Intensified Removal of Hydrogen Sulfide from Coke-Oven Gas in Rotary Hight-Speed Absorbers," *Zh. Prikl. Khim.*, **31**, 191 (1958)

Haug, H. F., Backmixing in Multistage Agitated Contactors—a Correlation," *AIChE J.*, **17**, 585 (1971).

Kirk, R. E., and D. F. Othmer, *Encycl. of Chem. Tech.*, Interscience, New York, **6**, 876 (1951).

Misaka, Y., "Studies on Removal of Hazardous Gas by Absorption," Doctor Thesis, Hokkaido Univ. (1967).

Sasaki, E., "Studies on Horizontal-Type Agitated Gas-Liquid Reactor," *J. Chem. Soc. of Japan*, Ind. Chem. Section, **74**, 799 (1971).

Takeuchi, T., K. Ando, and T. Osa, "Liquid-Phase Oxidation of Acrolein with Horizontal Stirred-Vessel," *J. Japan Petroleum Inst.*, **19**, 1022 (1976).

Tamaki, Y., and S. Ito, "Power Characteristics of Horizontal Shaft Agitator," *Kagaku Kōgaku*, **37**, 725 (1973).

Tamaki, Y., E. Harada, and S. Ito, "Interfacial Area and Surface Renewal Rate in Horizontal Shaft Agitating Gas-Liquid Contactor," *ibid*, **38**, 601 (1974).

Tamaki, Y., E. Harada, and S. Ito, "Transition of Annular State in Horizontal Agitated Vessel," *Kagaku Kōgaku Ronbunshu*, **1**, 75 (1975).

Ullmann, F., *Enzkl. der Tech. Chem.*, 2nd ed., Urban and Schwarzenberg, Berlin, **1**, 339 (1928).

Manuscript received December 3, 1979; revision received May 28, and accepted June 17, 1980.